(Contributions from R.W Kadel, Daryl Oshatz, Joseph Rasson, Craig Peters, S. M. Dardin)
LBNL, Version 2.0, July 30, 2001

1 Constraints

Integration of the DIRC into the BaBar detector is complicated by the requirement that the fused silica bars must pass through the flux return steel of the solenoid magnet. Complete azimuthal coverage of the active volume of BaBar by the DIRC is inconsistent with the support of the iron end-plug it surrounds. Hence, the mechanical design of the DIRC is a compromise that obtains the maximum azimuthal coverage while maintaining a conservative engineering approach to restraining the iron end-plug against gravitational and magnetic forces. Ultimately the DIRC covers 94% of the azimuthal area and the magnetic forces are carried by 12 uniformly spaced, thin, steel septa that divide the azimuthal coverage into 12 equal regions.

The mechanical support of the DIRC within the active volume of the detector $25.5^\circ \leq \theta \leq 141.4^\circ$ should be less than the fused silica radiators when measured in radiation lengths ($13.8\%X_0$), and should be as uniform as possible to reduce systematic effects in particle identification and the energy response of the electromagnetic calorimeter. The radial thickness of the DIRC was limited in this region to to 80 mm, leading to extremely tight mechanical toleances without much clearance for installation or seismic motion; implying a stiff, lightweight structure. This was ultimately accomplished by using air-craft type construction employing thin aluminum skins glued to the surface of lightweight foam or honeycomb panels.

Full coverage of the calorimeter in the forward direction required that the DIRC support be cantilivered from the backward end of the detector, with the obvious correlary that the DIRC also support the Drift Chamber (0.68 Tonnes). Rails and features on the inside of the DIRC support allow the support and removal of the endplug, necessary to service the the Drift Chamber electronics. Access to the Drift chamber inside the radius of the DIRC (0.8 m) was verified by construction of a full scale model of this region, including accelerator components that partially obstruct access through this cylindrical volume.

This structure must also support the Stand-Off-Box (SOB) containing 6 Tones of water used to interface the ends of the fused silica to the photomultiplier tubes. To protect the DIRC photomultiplier tubes and PEP-II accelerator components from stray magnetic fields the DIRC mechanical structure incorporates a “bucking” coil with special mechanical constraints.

The water of the standoff box represents a major safety concern as a water leak from the SOB into the calorimeter has the potential to destroy the CsI crystals of the EMC. Hence the DIRC mechanical design incorportates channels to direct water away from the calorimeter, to allow the early detection of leaks, and to quickly drain the SOB water inventory. Similarily, condensation from a water leak or changes in

dew point on the surface of the fused silica bars would destroy the total internal reflection necessary to transport the Cerenkov light down the length of the bars. Hence, the bars are kept in a continously flowing, dry nitrogen atmosphere.

To allow staging of the construction, and ease of repair, the 144 fused silica bars of the full DIRC detector are arranged into twelve nearly identical modules or "barboxes" that roll into the mechanical support analogus to file drawers in a cylindrical filing cabinet. Fabrication and assembly of the $\sim$ 5m long barboxes into the mechanical support with only 1 mm of radial clearance between the barboxes and their support was another of the major challanges of the mechanical design. The modularity of the barboxes meant they could be installed reletaively quickly into BaBar, with only the water seal and gas supply and return lines to be completed after the barboxes were slid into place. Below we describe in detail the mechanical support of the DIRC, the construction of the barboxes, gluing of the fused silica bars into final assemlies and their installation into the barboxes, as well as the installation of the barboxes into the support assembly. We conclude this section with a discussion of the gas system and water leak detection system.

2 Design Approch

The most basic requirements for the overall disign of the DIRC were that it be contained within an envelope of no more than 80mm of radial space in the active region of the detector. The 80mm radial extent includes a 1 mm tolerance for combined sum of deflection, alignment, and fabrication tolerances. There is an additional 5 mm stay-clear region between the DIRC and its neighboring components to allow for motion in response to a credible earthquake threat.

Mechanically, the DIRC was divided into two major peices, with the SOB, including photomultipliers and related electronics, and magnetic shield consisting of one comonent. All the remaining structures comprise the second component, including the mechanial support of the entire DIRC, support of the fused silica bars, and the interface between the quarz bars to the water in the SOB. The mechanical interface between the two halves of the projects is via a single Assembly Flange (AF) which incorporates all the mechanical fasterners, precision alignment features, and water interface between the two sub-assemblies.

Within the mechanial support, the DIRC may be sub-divided again into three major components: 1) the Strong Support Assembly (SSA) that withstands the gravitational and magnetic, and earthquake loads of the entire DIRC; 2) support of the barboxes in the active region of the detector (Central Support Tube, CST and

Transition Flange, TF); and 3) the fused silica bars and their local support in the Barbox modules.

3 Mechanical Support

3.1 Support Structure Assembly

With an overall height of over 6.7m, a mass of over 30 Tonnes, and numerous features with fabrication tolerances less than $250\mu m$, the DIRC Support Structure Assembly (SSA) contains a level of mechanical precision unusual for structures of its considerable size and weight. The SSA design was driven by a diverse set of functional and structural requirements resulting from its support of DIRC and other subsystem components as well as its position in the detector; embedded within the backward end of the Flux Return Assembly. These requirements necessitated careful mechanical design, extensive engineering analysis, and specific fabrication and assembly procedures. Figure 1 showes an exploded view of the SSA.

3.1.1 Design Constraints and Requirements

The SSA and CST contain precisely aligned rectangular slots for Barboxes and tracks that guide the boxes during insertion and hold them in their final $x - y$ positions. The Barbox slots were machined and each SSA component aligned during assembly such that adequate clearance for installation was maintained along the length of each slot. The Barbox tracks in the SST needed to be precisely machined and located to ensure smooth running of the Barbox wheels and cam-followers and alignment with the aluminum tracks that extend into the CST.

The radial clearance, nominally only 5 mm, between the outside diameter of the CST and the inside diameter of the electromagnetic calorimeter calibration system, imposed stiffness and alignment constraints on the CST and the SSA, which supports the CST as a cantilevered load. Although the total mass of the CST loaded with barboxes is small, approximately 1.6 Tonnes, the small radial gap necessitated detailed structural analysis to ensure that no collision could take place due to static deflection or a probable seismic event.

The SOB is supported as a cantilevered load off of the backward end of the SSA. With a total mass of 15 Tonnes and lower stiffness than the SSA, the SOB constitutes a significant static load on the SSA. Prior to detailed FEA analyses, there was some concern that the SOB could act as a resonator during seismic events that could drive large displacements of the free end of the CST.

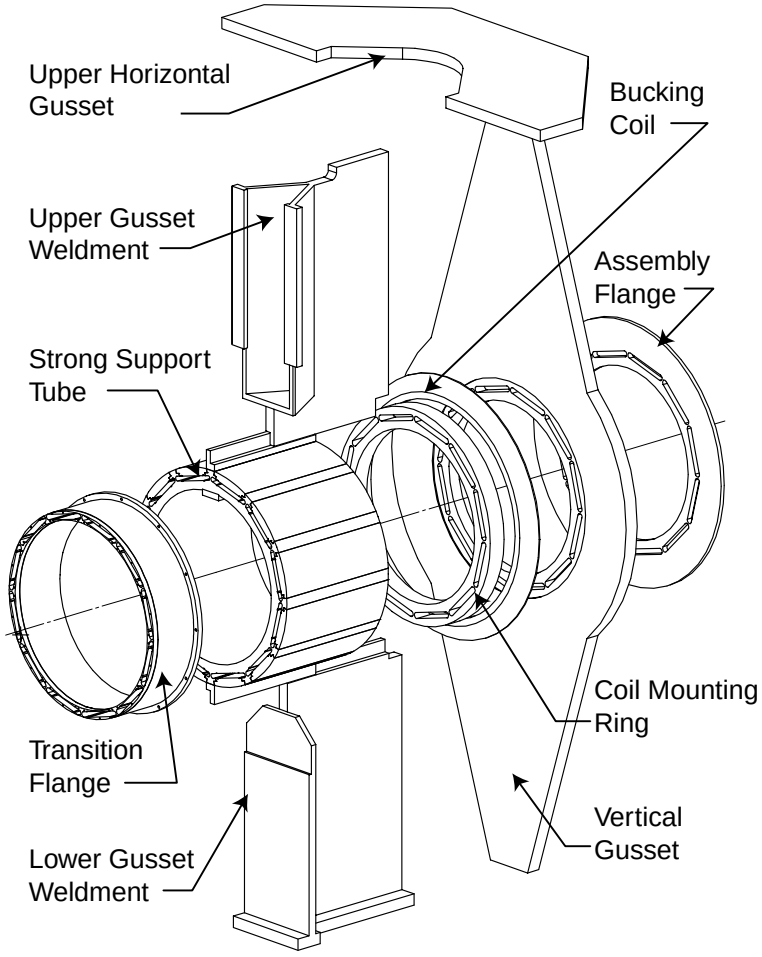

Figure 1: Exploded view of the Strong Support Assembly. Missing from the figure are the Stand Off Box in the rear, and the Central Support Tube in the front.

The SOB water seals are made to the Assembly Flange (AF) on the SSA. The AF contains twelve O-ring grooves for Barbox diaphragm seals as well as two polished O- Ring surfaces for the large diameter seals to the outer cone and inner cylinder of the SOB. In the even of a water leak in one of the barbox diaphragm seals, drainage passages plumbed into the Coil Mounting Ring (CMR) would allow water to escape before hydrostatic pressurization of the CST Barbox liners occurs.

The inclusion of the Bucking Coil in the SSA complicated the design and assembly of the overall structure. The coil required a non-magnetic mounting ring. Because the SST is carbon steel, it was made shorter and the stainless steel CMR was included in the assembly. In order to facilitate disassembly of the SSA for repair or replacement of the Bucking Coil, the upper and lower gussets are bolted, rather than welded, to the large vertical gusset (VG).

3.2 Static and Magnetic Loads

The SSA and the backward endplug, which it holds in place, are part of the flux return path for the super-conducting solenoid. The SSA resists 210 tons of magnetic force tending to pull the Strong Support Tube (SST) and backward endplug towards the I.P. The backward endplug is a cylindrical assembly made from low carbon steel with a total mass of approximately 11.3 Tonnes. The assembly consists of two pieces; a semi- circular lower portion and horseshoe-shaped upper portion. The lower portion is bolted into the SST Inner Cylinder at the five o-clock and seven o-clock locations. The upper portion is removable for service access and is mechanically restrained by the lower portion and a steel plate, referred to as the Plug Stop, bolted to the inside diameter of the SST Inner Cylinder at the twelve o-clock location.

The Drift Chamber is supported inside the CST at its forward and backward ends. The Drift Chamber's forward end flange is held in position with twelve radial supports; two adjustable struts and ten shims. With a mass of approximately 0.7 Tonnes, the Drift Chamber also contributed to the static deflection of the CST due to gravity.

The SSA's physical location in the BaBar Detector imposes spatial constraints in addition to those already discussed. The backward doors of the Instrumented Flux Return (IFR) assembly close around the SSA with a nominal clearance of only 10 mm to the SST and gussets. Once these doors are closed, access to the structure is completely blocked. The Bucking Coil and CMR water plumbing were designed to stay clear of the path of the inner corners of the doors which open and close at a five-degree angle. The tirangular chimney for the cryostat of the Superconducting Solenoid restricted the bolting locations available on the Flux Return

upper mounting plate to two narrow strips on either side of the chimney. In general, the locations available for bolting the SSA to the Flux Return were largely limited by its location, embedded within several other assemblies.

3.2.1 SSA Design and Fabrication

The fundamental challenge in designing the SSA proved to be balancing the need for high precision in the Barbox slots with the stiffness and strength requirements imposed by magnetic forces, seismic loads, and limited clearances around the structure.

The Barbox slots in the SSA pass through five separately machined components made from three different materials, bolted and pinned together. The goals of maximizing septum thickness and Barbox clearance drove the tolerances for slot machining and alignment of all components. The material between two slots is referred to as a septum. Twelve septa, each less than 15.2 mm thick, connect the inside of each cylindrical part to the outside. Early in the design process the possibility that magnetic forces would create high stress in the septa was recognized. The azimuthal quartz coverage requirement and the need for Barbox insertion clearances limited the amount of material that could remain in the septum area. Every effort was made during the design process to maximize the septum thickness and, thereby, minimize stress. Because failure in one septum could catastrophically increase the stress in others, the strength of these septa was deemed to be of critical importance to the structural integrity of the DIRC structure and, therefore, the backward end of the BaBar Detector.

The Strong Support Tube (SST) consists of a continuous inner cylinder and an outer cylinder comprised of twelve plates. The septa connecting the inner and outer cylinders are machined into the inner cylinder, a carbon steel forging. These septa, each approximately 1143 mm in length, transfer approximately 170 tons of magnetic force from the inner cylinder to the outer cylinder. The SST is the primary strength member in the SSA, resisting radial and bending forces that tend to put the forward end of the SSA in tension and the backward end in compression. Figure 2 shows the details of construction of the SST.

The Barbox slots in the SST contain track features in which the Barbox wheels ride during insertion. In order to ensure proper fit and guidance of the wheels, the track features were machined to a unilateral profile tolerance of 0.1 mm. The Barbox slots in the SST were machined to a unilateral profile tolerance of 0.25 mm. These tight tolerances, the overall length of the assembly of 1149 mm, and the narrow radial width of the slots of only 41 mm, precluded machining the slots and tracks

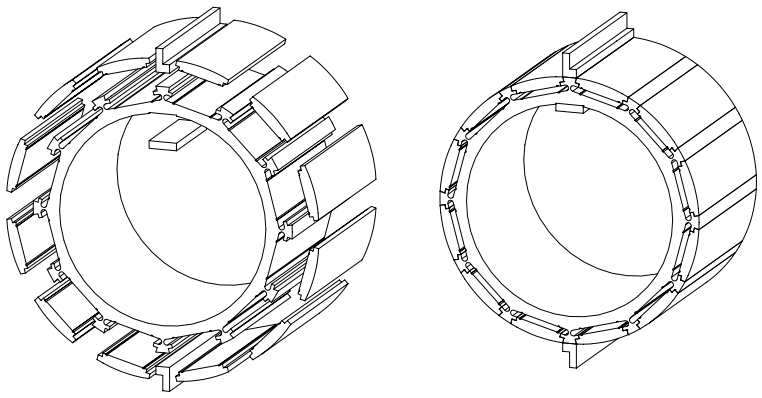

Figure 2: a) Exploded view showing the construction of the steel of the SST and b) assembled part.

in a continuous steel ring with conventional or wire EDM techniques.

The Outer Cylinder Segments of the SST are bolted and pinned in place on the outside of the Inner Cylinder. This design allowed precise machining of all features inside the slots with conventional machining techniques. Each Outer Cylinder Segment was aligned to its respective Inner Cylinder slot with tooling which indexed the tracks in both parts. Once the segments were aligned they were bolted in place and match-drilled and pinned. These bolts and shear pins holding the segments in place maximize the radial stiffness of the assembly.

All components of the SST were electroless plated with 25μm of nickel. This plating provides a tough, corrosion resistant bearing surface in the Barbox wheel tracks. The option of selectively plating the track surfaces and painting other exterior surfaces was explored and dismissed because of the availability of plating tanks of adequate size to accommodate the Innner Cylinder. Given the proximity of deionized water in the SOB, rust resistance was deemed to be of critical importance.

The Transition Flange (TF) was fabricated as part of the SSA because of the need to achieve precise alignment of Barbox tracks in the CST with respect to the tracks in the SST. The CST and SSA were fabricated concurrently, the CST at LBNL and the SSA in Kobe, Japan by Kawasaki Heavy Industries (KHI). The TF was machined with a matching aluminum template as the first component in the SSA assembly. The TF was then shipped to LBNL so that the CST fabrication could begin while the SSA machining continued at KHI. The aluminum template remained at Kobe and was subsequently used during the acceptance tests to demonstrate proper alignment of the TF slots with respect to slots in and the rest of SSA.

The Transition Flange is a thick wall cylinder about 500 mm long and 1780 mm in diameter, machined from a single piece of a rolled ring forging of aluminum 6061-T6 alloy. The slots were machined from either end of the ring to a unilateral profile tolerance of 0.5 mm. The slot dimensions and profile tolerance were larger than that for the slots in the SST and other SSA components, achieving a clearance fit with the slot liners of the CST. The slot liners assemblies containing the CST Barbox tracks were subsequently aligned in the TF slots to match the tracks in the SST.

The low-radiation-length, composite portion of the CST was made slightly longer than physics requirements necessitated in order to decrease the length of the TF. With a total length of 505 mm, the TF extends 135 mm short of the active region of the detector. This length was selected to facilitate fabrication of the TF from a single forging with conventional machining techniques. A detailed finite element analysis of the DIRC structure [1] indicated that the additional length of composite structure had an acceptably small affect on stiffness.

Two dowel pins, located in the six and twelve o-clock positions, align each cylindrical component to the next. The Barbox slot features in all parts were located with respect to the dowel pin holes. A carbon steel template was utilized to establish the position of the slots and alignment holes during machining of the steel and stainless steel parts. This template was fabricated with slots having a profile tolerance of 0.05 mm and locating holes with a true position tolerance of 0.1 mm.

The slots in the AF, VG, and CMR do not contain Barbox track features. The VG and CMR slots were machinined to a unilateral profile tolerance of 0.5 mm. The AF slots were machined to a tighter tolerance of 0.25 mm in order to assure adequate thickness of the thin wall of material between the O-ring grooves for the Barbox diaphragm seals and the slots in the septum area.

The VG, Upper Horizontal gusset (UHG), Upper Gusset Weldment (UGW), and Lower Gusset Weldment (LGW), were fabricated from carbon steel plate (ASTM A-36). The interface surfaces between the gussets and the VG were machined to a tolerance from 0.1 mm to 0.25 mm to ensure continuous contact in bolted connections. In order to achieve these tolerances and the long-term stability of the assembly, all parts were stress relieved prior to final machining.

To facilitate disassembly for access to the Bucking Coil the UGW and LGW are bolted and pinned to the SST Gusset Backets, which are bolted and pinned to the SST Inner Cylinder. These bolts and shear pins transfer the considerable shear forces caused by magnetic loads on the SST and Backward Endplug.

The upper portion of the LGW mounting flange overlaps the outer radius of the super- conducting Solenoid. In order to avoid affecting the shape of the magnetic

field, a non- magnetic stainless steel plate forms this portion of the flange.

The DIRC structure is held onto the Instrumented Flux Return (IFR) by bolts passing through custom machined alignment shims and mounting holes in the SSA. The mounting holes in the UGW and LGW were drilled 5 mm larger than the diameter of the mounting bolts. This 5 mm accommodated alignment clearances and machining tolerances. In order to maximize the amount of clearance available for adjustment of the DIRC structure during installation, the holes were toleranced to a true position of 1.0 mm with respect to datums on the assembled structure. The final location of the thread inserts in the mounting plates on the IFR was measured at SLAC. These measured locations were used as the nominal locations for the mounting hole drilling in the UGW and LGW at KHI. The high precision of the gusset weldments, the SST Mounting Brackets, and the VG, enabled KHI to meet the required tolerance by machining the mounting holes in the gusset weldments prior to final assembly. Because the UHG is designed primarily to brace the DIRC during seismic events, a larger clearance of 10 mm was selected for its mounting holes.

3.3 Assembly and Acceptance Tests

The SSA assembly was performed with the SST facing downwards. Dowel pins were installed to align each pair of components containing Barbox slots. During the assembly the Bucking Coil was temporarily supported from brackets bolted into the CMR drain ports. A detailed half-symmetric finite element model of the DIRC structure was utilized to analyze the stresses and deflections resulting from gravitational, magnetic, and seismic forces. Figure 3 Shows the deflection of structure. The maximum stress (Fig. 4) was predicted to occur within a septum in the Vertical Gusset.

3.4 Experimental Validation of FEA Predictions

During the month of April 1998 measurements were made of the stresses in the DIRC Strong Support Tube (SST) caused by magnetic forces. The objective of these measurements was to confirm the safety of the DIRC Support Structure was designed to withstand loading with the solenoid at a field strength of 1.5 Tesla. The measurements focused on the forward end of the SST in the thinnest regions of the steel at the septa.

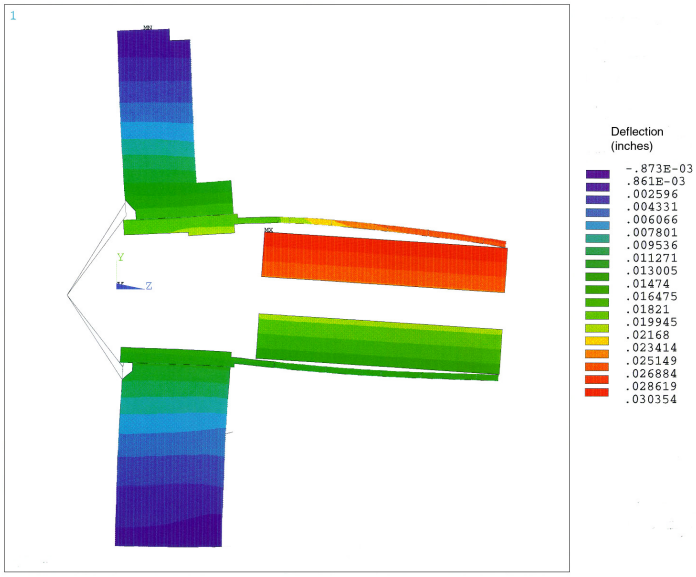

Figure 3: Deflection of the strong support structure and the CST under the combined magnetic and static gravitional loads, including the DCH. The amount of deflection of the structure has been exagerated for clarity. This FEA calculation models the effect of the fully loaded SOB as a applied vertical load at the intersection of the dotted lines at the left of the figure, rigidly attached to the assmebly flange.

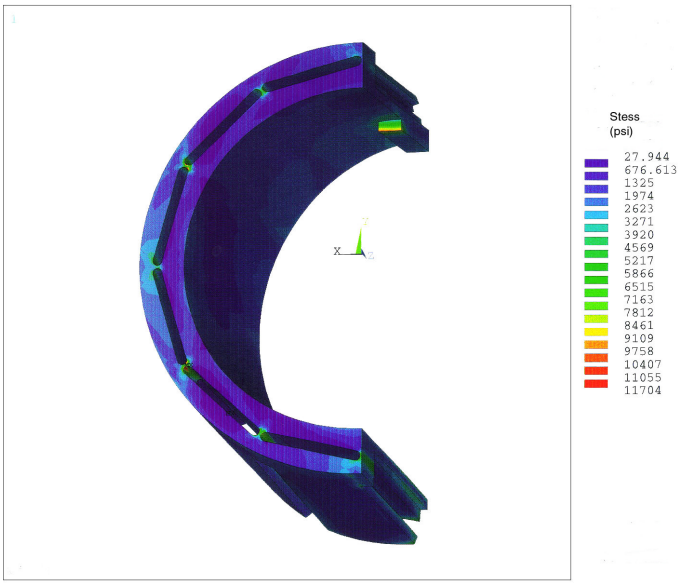

Figure 4: Stress diagram in the of the strong support tube under the combined magnetic and static gravitional loads, including the DCH. The maximum stress occurs in the septum at ∼8 o'clock.

3.5 Central Support Tube (CST)

The Central Support Tube (CST) is a cylindrical assembly of 1780 mm diameter and 3350 mm length. The radial thickness of the CST is 75 mm. Several components make up the CST as shown in figure 5 Transition Flange which is a rigid flange for mounting the CST to the SSA, a light weight cylinder section attached to the Transition Flange made up of 12 I-Beams and 12 barbox slot liners, and an aluminum skin bonded to the inside and outside of the CST frame. The slot liners incorportate the track details for the barboxes, and are continous throught the transition flange and the CST.

The CST is mounted horizontally within the Babar and its primary function is to support and accurately position the barboxes within the active region of the detector.

It is necessary that the CST have a low Z mass and be mechanically rigid. Additionally, the barbox liners must be straight and accurate profile, as desribed below. The CST needs to be mechanically stiff so that it stays within the allocated space envelope within the detector. The CST is in effect a cantilevered beam since it is supported only at the backward end of the detector. The CST supports the mass

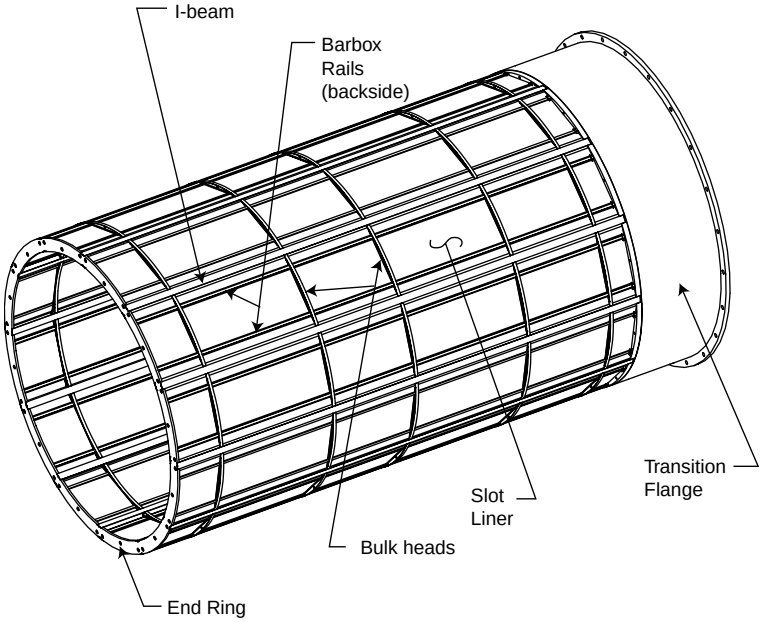

Figure 5: Schematic diagram of the CST and transition flange. The outer aluminum skin is missing in this view to show the internal construction of I-beams, bulkheads, barbox slot liners.

of the Barboxes - about 1.6 Tonnes pounds, and the forward end of the CST supports half the 0.7 Tonne mass of the drift chamber. The small radial clearance between the outside diameter of the CST and the inside diameter of the EMC calibration system requires that the CST outside surface be within 1 mm of its nominal design surface. Fabrication tolerances as well as deflections due to gravity were required to be within this tolerance.

The CST cylinder is constructed similar to a semi-monocoque airplane wing in that it has internal I-Beam stringers and bulkheads over which a thin skin is bonded on the outside and inside. The final assembly and skinning of the CST was done with the cylinder in the vertical orientation so that gravity would not cause distortion or complicate the alignment process. The skins provide most of the strength and stiffness of the CST cylinder.

3.5.1 CST Fabrication and Assembly

In general, most of the CST elements are bonded together - mechanical fasteners are not relied upon to carry load. A single type of commercially available 2-part epoxy adhesive was used throughout the CST. The chosen epoxy[4] has a high peel strength ($\geq$50 pli or $\geq$90 Nt/cm) and a 4500 psi (3×10^7 Nt/m^2) tensile lap shear strength which are excellent strength values for this application. The epoxy was dispensed from cartridges through a mixing nozzle and could be applied to vertical surfaces without sagging due to its thixotropic property. A 24-hour room temperature cure produced a 90% strength bond. Glue line thickness was controlled through 125 μm diameter glass beads contained in the epoxy components before mixing. All bonded components were aluminum and were cleaned to LBL UHV cleaning standards. Clean procedures were used through out assembly sequence to maintain part cleanliness.

3.5.2 Barbox Liner Design and Fabrication

The CST contains 12 barbox slots that line up with 12 slots that go through the SST cylinder. Each of the barbox slots in the SST and the CST contain 4 tracks. Wheels on each barbox engage these tracks as the barbox is rolled horizontally into the slots. Minimal clearance (1 mm) exists between the barboxes and the slots in the CST. It is necessary for the slots to be dimensionally accurate and to be accurately located with respect to the SST slots so the barboxes will roll in without interference or dragging in the slots and without hitting any step at the SST/CST interface. The CST tracks were required to be positioned to a 0.4 mm zone with respect to SST

features.

The barbox liners consist of extruded 6063-T6 aluminum track sections screwed and bonded [2] to 2 flat and 2 U-shaped sheet metal sections to form the rectangular liner section. During the assembly of the liners the 4 tracks were held straight and in accurate position by fixturing while the sheet metal sections were match drilled and bonded.

Lightweight (170 gram) bulkheads were CNC machined from aluminum plate. The bulkhead function is to support the barbox liners inside the CST. The bulkheads are bonded onto the barbox liners while the liner internal fixture is still inside the liners. Bulkheads were 100% inspected and were required to be nominal size $\pm 25\mu$m. During bonding the bulkheads are positioned and aligned with respect to each other by fixtures mounted on a granite table. Figure 6 is a cross section through the CST, showing the details of the end of the CST opposite the transition flange.

3.5.3 CST Assembly

The Skins provide most of the strength and stiffness of the CST cylinder. Inner and outer skin thickness was 1.27mm (0.05 inch) and 0.76mm (0.030 inch), respectively. The I-Beams were 100% inspected for cross-section and straightness. The one exception to the no fastener approach for the CST is the I-Beam connection to the Transition Flange. The end of the TF was slotted about 75mm deep into which the I-Beam webs were inserted. The flanges of the beams were then screwed and bonded to the TF[3]. The Barbox Liner Assemblies were then slid in between I-Beams using alcohol as a lubricant. The CST end flange was attached to the I-Beam ends and then aligned using fixture struts so that the CST formed a true cylinder. The free end (or end flange end) was aligned with the TF base of the CST cylinder Epoxy[3] was then injected into the I-Beam to Bulkhead joints through injection holes.

The inner and outer CST Skins were each divided into six 60° arcs. An inner and outer skin section were then clamped to the CST frame using a "skinning" fixtures. These fixtures were fabricated by aligning the fixture parts on a surface table and then bonding all the parts of the frames together. This produced straight skinning fixtures with very accurate profiles that enabled the CST skins to be bonded while the CST shape was being held as a true cylinder. The skinning process was repeated for each of the six pairs of skin segments. Prior to each new pair of skin segments be bonded, the free end (End Flange) was realigned with the TF at the base of the CST cylinder. A consistent glue line thickness of 0.38mm (0.015 inch) inch between the skins and the frame was maintained by burying wires of that thickness in the glue line [4].

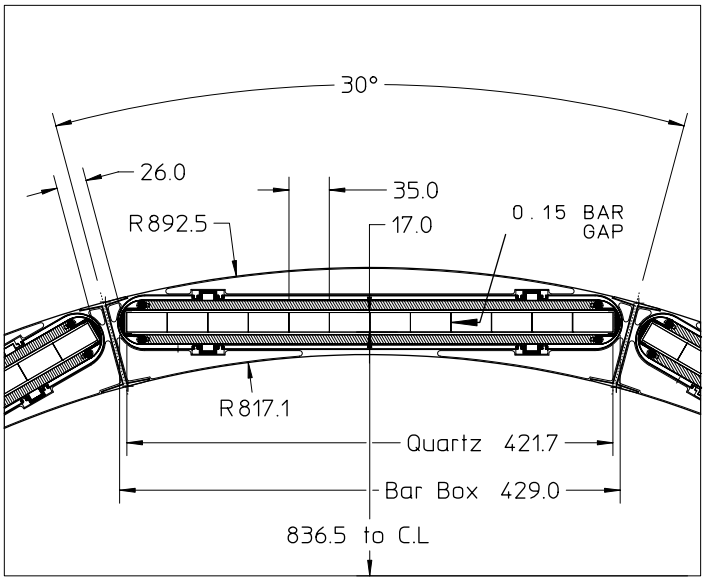

Figure 6: Cross section though the CST showing a bulkehead, the slot liner and a babox. The inner and outer skins of the CST are not shown.

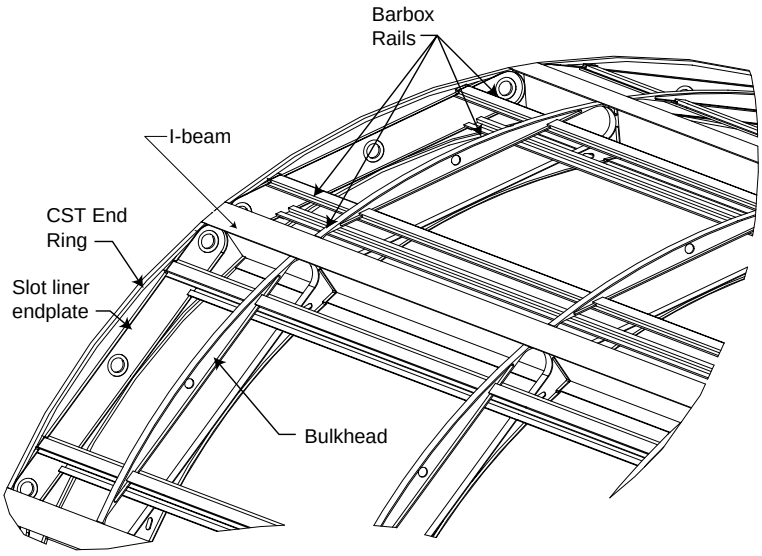

Figure 7: Details of the CST assembly near the end opposite the transition flange. The inner and outer skins have been removed, as well as the four peices of stainless Steel sheet metal that form the slotliners when bolted to the rails. The rails and slot liners extend all the way through the transition flange.

The critical joint in the CST is the tie in of the lightweight cylinder section to the TF. The I-Beams and the skins share the shear load carried by this joint. The I-Beam joint is described above. The joint to the skins is a 75mm lap joint along the full circumference of the TF (approximately 0.85 m^2 or 1320 in^2), adequate to support 2.5 tonnes.

After bonding all the skin segments the alignment of the End Flange with respect to the TF was within 125μm. With the CST rotated to the horizontal orientation and cantilevered from the TF, the maximum radial runout at any position was 1.0 mm.

3.6 SOB, SSA, and CST Installation and Alignment

The installation of the DIRC into BaBar is complicated by the small clearances between the DIRC and the other BaBar sub-systems and the large physical dimensions and weight of the entire device. To install the DIRC a large fixture was constructed that could rotate the DIRC around three-axes or translate the DIRC in two transverse dimensions within comfortable limits anticipated for the initial

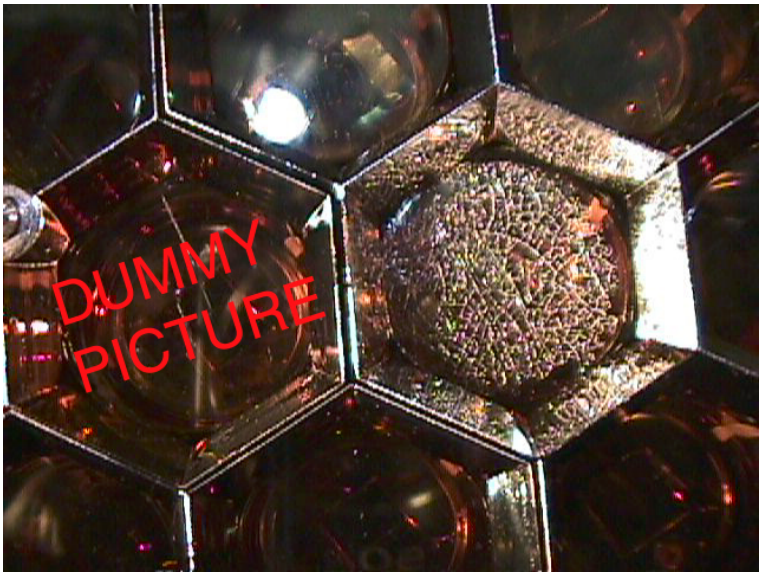

Figure 8: Picture of the installation figure for the DIRC showing the fully assembled SSA and CST. The Barboxes are not installed, and missing from the figure is the SOB, both of which can be accommodated in the installation fixture.

alignment. Figure 8 shows a picture of the installation fixture with the SSA and CST attached. In the z direction, the motion of the DIRC is obtained by rollers on a custom track, and its position in this coordinate controlled by hydraulic jacks. The fixture is designed so that it can also support the SOB, and if necessary the entire DIRC can be removed from BaBar on this platform. However, this requires the removal of the accelerator components and the Drift Chamber.

The DIRC was installed within 1mm of its expected position, based on optical survey measurements. Measurements of the bending and strains of the DIRC SSA and CST (taken without the Drift Chamber and SOB present) under combined gravitational and magnetic loads are consistent with expectations.

4 Barboxes

The design goal for the barboxes is to provide a clean, mechanically stable support for the bars that is as thin as possible when measured in radiation lengths. The Barbox provides the seal between the water of the SOB and interior of the barbox at the backward end of the detector. The volume inside the barbox must be reasonably

gas tight, to prevent condensation on the bars from destroying the total internal reflection of the Cherenkov light.

The 35mm × 17mm × 1.225m bars as received from the manufacturer are referred to as "short-bars" and "long-bar" refers to four short-bars and a wedge glued into a single, 4.9m long final assembly.

Ideally, the long-bars would be kinematically supported within the barboxes. However, because of their extreme length to width ratio, the long-bars must be supported at multiple points along their length. These supports are arranged keep each long bar in a straight line, minimizing any applied torque that might bend the bars or stress on the glue joints between the short bars. This is accomplished within the barbox by spring loaded top, end, and side load buttons push the bars against pricisely aligned, fixed bumpers. This support mechanism allows for differenital expansion of the silica and the mostly aluminum support, and provides resistance forces generated during transportation or a crediable earthquake.

A schematic diagram of a barbox are shown in Fig. 9. The barbox consists of three sections: a) the active region, b) the mirror end, and c) the window end, including the water seal. These regions are built mostly of aluminum honeycomb materials and thin extursions, or, in the case of the mirror end, solid alumimum peices that have been heavily machined to remove as much material as possible. The support of the bars must be spring loaded in all directions to account for the difference in thermal expansion between fused silica and the aluminum support sturcture under a temperature change of ±20°C, the maximum anticipated temperature variation during transportation and installation. The spring loading also insures that glue joints are generally kept in compression during normal handling, operation or earthquakes and that the bars do no move around inside the barbox during transportation.

The barboxes must be supported under a variety of load conditions, since the 429mm dimension can be rotated in any direction with respect to the direction of gravity. Within the CST and SSA the barboxes side into their slots on 16 wheels (or cam followers) that align with the four tracks of the CST and SSA. There are eight pairs wheels built into one cover of the barbox, and eight pairs of cam-followers on the opposite cover. The wheels and cam-followers are made out of similar parts, except the cam-followers rotate about an axis perpendicular to the axis of the wheel rotation.

For barboxes where the 429 mm dimension is mostly horizontal, most of the weight is carried by the wheels, and the cam-followers help guide the barbox into their slots. For the barboxes where the 429 mm dimension is nearly vertical, the role of the wheels and cam-followers is reversed, with the cam-followers carrying most of the weight. However, wedges at the backward, instrumented end always point

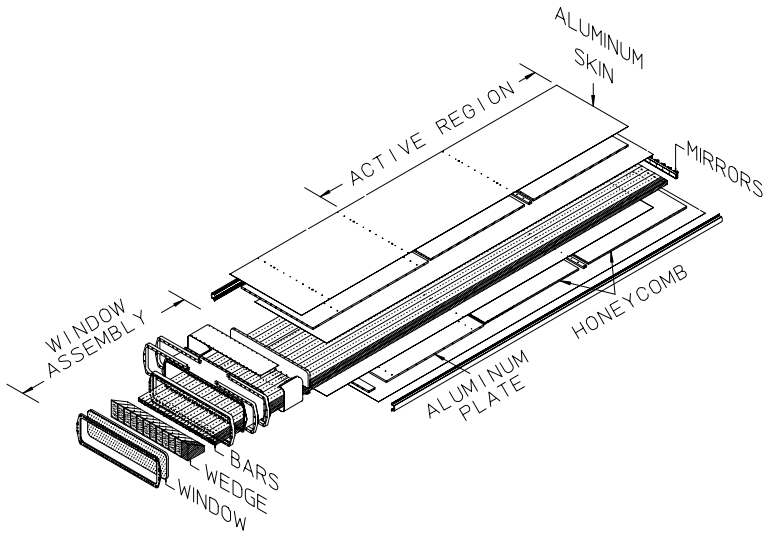

Figure 9: 3D schmatic drawing of a barbox showing the Active region, mirror end and window ends

radially outward. Therefore the barboxes are *almost* identical, with the exception that the cover with the wheels (or cam-followers) changes sides of the barbox with respect to the direction of the wedge depending on wheather it is in the lower half (barboxes 3-8) or upper half (barboxes 0-2 and 9-11) of the DIRC. A further mechanical complication due to the gas supply and return lines breaks the symmetry of the boxes in the vertical plane, and in fact, there are four distinct types of barboxes for the full detector.

Inside the barbox, the bars must be kept free from condensation. Nitrogen gas is routed in a small 3 mm diameter tube from the window end along the outside of the barbox to the mirror end, where it is introduced into the barbox. From there it flows along the bars back to the window end and exhausts into a return line for analysis (see the description of the gas system below). To avoid excess pressure inside the barbox, the gas pressure is set normally less than 20 mm water equivalent, and each barbox is equiped with a custom pressure relief value set to fully open at a pressure of 250 mm water equivalent.

4.0.1 Material Inventory and Radiation Lengths

Table 1 lists the materials used in the construction of the CST and the barboxes and the distribution of material as a fuction of ϕ from the center to one edge of a

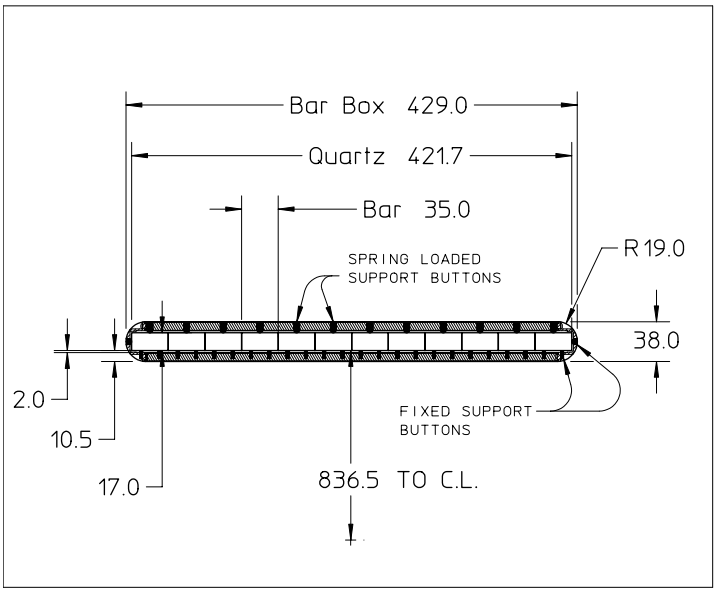

Figure 10: Cross Section of a Barbox in the active region of the detector.

barbox is shown in figure 11. There are two curves in the plot. The lower curve is the amount of material in front of the quartz bars due to the mechanical structure of the DIRC only. The upper curve is the material in front of the EMC due to the DIRC only. The structures in the plot between $8^\circ - 11^\circ$ are the rails for wheels of the barboxes. The structure between $12.5^\circ - 14.5^\circ$ is the Aluminum extrusion of the side rail. The sharp peak at phi=14.1° (upper curve only) is the end of the quartz, followed by another, equal peak due to the vertical wall (24 mm high) of the side rail of the barbox. Finally, the big peak (0.87 radiation lengths) at the right edge of the plot is the "web" of the I beam of the CST (solid aluminum) plus the inner and outer skins.

In table 1 and figure 11 only things in the DIRC that are continuous in z are included. Missing are "lumped items" such as bulkheads, wheel supports, mirrors, barbox endplate, endplate to the slot liner, and the CST endflange are listed in table 2. These descrete items add another 0.016 X_0 to the average thickness of the DIRC mechanical sturcture, with about half this material before the bars.

The minimum material in front of the fused silica bars and the EMC occurs at $\phi = 0$ and is 2.7% X_0 and 18.7% X_0, respectively. The average material in front of the bars and the CST is 3.7% X_0 and 20.7% X_0, respectively, incluing the distributed items of table 2. An infinite momemtum partitle from the IP passing through one half the thickness of the fused silica bars in the forward, end-ring region of the DIRC would tranverse 0.35 of a radiation length.

The details of the active region, the mirror end and the window end of the barbox are discussed below.

4.0.2 Active Region

A crossection through a barbox in the active region of the detector is shown in Fig. 10. The support of the "short-bars" within the barbox assembly is designed so as to minimize the force on the glue joints of the "long-bar" assemblies. To minimize the force on the glue joints, the short-bars are supported such that under their own weight, the ends of the short bars would be in a vertical plane. This condition is satisfied when the supports are located a distace $z = 0.211L$ from each end of the short-bar, where L is the length of the short-bar. The sections of the load buttons and bumpers in contact with the bars are made from nylon or teflon, and were extensively tested to assure that they do not damage the surface of the bars.

In the direction perpendicular to the 429 mm $r\Delta\phi$ dimension of the barbox, the bars are pressed against two fixed nylon buttons by a sring loaded bumper on the opposite side of the bar. This combination of spring loaded bumper plus two

Table 1: List of components used to construct the CST and Barboxes, their dimensions and thickness in radiation lengths. Glue and plastic parts are not included. The coordinate system is measured in the barbox reference frame, with y parallel to r at $x = 0$, where x is in the $r \times z$ direction. Dimensions (mm) with brackets (<>) indicates average values for complicated shapes. The number of radiaton lengths is the average for each component as traversed by an infinte momentum tracks over the range $0^\circ \leq \phi \leq 15^\circ$ and $\theta = 0$

Component	x_1	x_2	y_1	Δy	Material	X_0
CST I-SKIN	0.00	218.59	815.79	1.27	Al	0.0143
Rigid foam[1]	0.00	214.50	817.10	37.50	Urathane	0.0002
Slot I-Liner	0.00	126.71	821.30	0.40	Al	0.0045
BB Skin1	0.00	195.00	825.60	0.25	Al	0.0029
BB Honeycomb[2]	0.00	195.00	825.80	8.40	Al	0.0024
BB Skin2	0.00	195.00	834.20	0.25	Al	0.0029
Fused Silica	0.00	210.07	836.50	17.00	SiO_2	0.1383
BB Skin3	0.00	195.00	855.70	0.25	Al	0.0029
BB Honeycomb	0.00	195.00	856.00	8.40	Al	0.0024
BB Skin4	0.00	195.00	864.40	0.25	Al	0.0029
Slot O-Liner	0.00	126.71	868.00	0.40	Al	0.0045
Rigid Foam	0.00	214.50	868.70	37.50	Urathane	0.0002
CST O-Skin	0.00	239.14	892.50	0.76	Al	0.0085
Rail Inner	126.71	154.04	818.80	$< 4.55 >$	Al	0.0500
Rail Outer	126.71	154.04	866.20	$< 4.55 >$	Al	0.0500
CST Beam	198.64	238.62	817.10	$< 8.92 >$	Al	0.1003
Side Beam	195.00	214.27	827.50	$< 6.95 >$	Al	0.0781

[1] density = 0.0687 g/cm^3
[2] density = 0.0478 g/cm^3

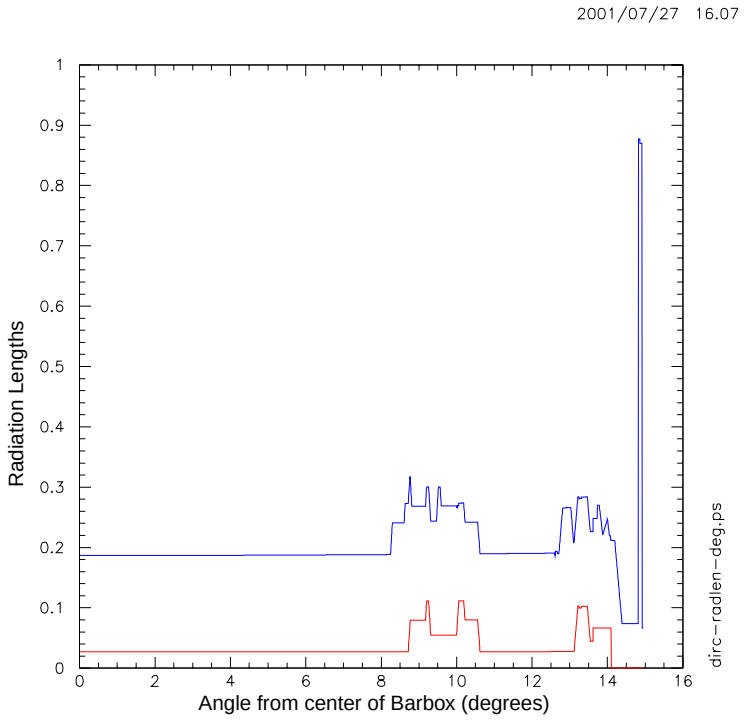

Figure 11: The amount of material in the DIRC as a fuction of the angle from the center of a barbox for an infinite mometum track from the IP at $\theta = 0$. The material thickness is measured in radiation lengths, and includes both materials in the CST and the barbox. The lower curve is the material in front of the fused silica bars due to the mechanical structure of the DIRC, and ends at an angle of 14° with the edge of the bars. The upper curve is the amount of material in front of the EMC due to the DIRC. This curve stops at 15°, a 12-fold symmetry axis of the DIRC.

Table 2: List of descrete items in the DIRC mechanical sturcture not included in Table 1. They are divided into two classes: 1) bulkheads and wheel supports in 5 rings distributed along the entire DIRC coverage, and 2) items at the forward (unstrumented) end of the DIRC at $\sim \theta = 25.5°$. The average radius of all items is 845 mm. The mean radiation length is for an infinte momentum track from the IP. Dimensions with brackets (<>) indidicate average values for complicated shapes.

Component	Material	Δz	Δr	$r\Delta\phi$	ϕ Coverage	Mean X_0
Distributed items						
Bulkheads	Al	8	75.4	442	1.0	0.0042
Wheel supports	Al	25	16.4	390	0.881	0.0103
Forward Items						
Mirrors	SiO_2	3	17	414	0.935	0.0253
HC Termination	Al	20	15.0	390	0.881	0.0015
BB-Rear Cover	Al	< 8.72 >	38	432	0.976	0.1060
SL-endplate	Al	< 3.6 >	51	435	0.983	0.0441
CST end Ring	Al	< 5.02 >	75.41	-	1	0.0625

opposing buttons is repeated at eight locations along the length of the long bar for the reasons described above. The height of the fixed bumpers was set to $\pm 25\mu$m by suspending the cover a known distance above a flat, granite table and pressing the bumpers against the surface of the table. The bumpers were then glued [5] into place under vertical load to keep them in contact with the granite surface as the glue cured. The fixed bumpers are threaded on their circumference to provide a good mechanical joint between the plastic bumper and the aluminum cover.

Threaded nylon bumpers are also used to support the bars from the extruded aluminim side rails (*i.e.* forces parallel to the 480mm dimension). The flexing of the side rails due to the load applied through the bumbers supplies is large enough to supply the spring load for the bars in this ($r\Delta\phi$) direction.

Maximizing the geometrical acceptance of the bars implies minimizing the separation between the bars within a barbox. The bars must lie as close as possible, but not bump into each other. Loads applied perpendicular to the length of the bars must align with supports, because the bending of the bars under an applied torque as small as 1.5 Nt-m, offset by 10 mm from the nominal support point in the z direction, will cause neighboring bars to touch between the support points. The bars are separated from each other by shims made of folded 50μm aluminum foil (see below)

4.0.3 Mirror End

Cherenkov light from tracks in the forward direction requires a mirror at the forward end of the long bars to refect the forward going Cherenkov light to the backward, instrumented end. At the front surface of the bar a spring loaded, front surface, mirror with an aluminum coating is placed against the end of the bar, without glue or coupling compond, to reflect the Cherenkov light back to the instrumented end. The mirror assembly is shown in figure 12.

The reflectivity of the mirror is about 95% in the wavelength region of interest for the DIRC.

The load applied to keep the mirror next to the end of the bar must satisfy two additional, complementary requirements. The load must be high enough to resist earthquake loads (up to 1.6 times the weight of the bars), and keep the glue joints in compression. Additonally, this spring load, tranmitted from the mirror end to the window end via the bars, helps to support the window against the pressure of the water in the SOB, about 150kgf for boxes 5 and 6 at the bottom of the detector. The assembly procedure for installing the mirror is described below.

4.0.4 Window End

At the window end of the barbox, inside the volume defined by the SOB, the barbox is expanded outward in the radial dimension to create a enclosed volume for the wedges. All 12 wedges are glued to a common 10 mm thick fuzed silica window that forms the interface between the silica bars and the water of the SOB. The window itself is captured in a stainless steel window frame and made water tight by rubber gaskets that are compressed on both its forward and backward surfaces. All fasteners exposed to the di-ionized water inside the SOB are gold plated stainless steel. The window frame is attached to the barbox via a stainless steel "wedge cover", a sheet metal assumbly, fabricated from six parts joined with epoxy glue backed-up by metal screws. These parts are added to the barbox assembly after the window has been glued to the wedges (see below). The wedge cover, and hence the barbox and the slot in which the barbox rests, is kept water tight by a custom made, EPDM rubber diaphram which seals to gooves cut in the window frame and the assembly flange of the SSA. Details of the window end of the barbox are shown in figure 13.

All the barboxes were pre-assembled without bars, and the peices match marked. The two aluminum extrusion side rails were glued [5] to the lower cover, as well as the fixed bumbers and wheel/cam assembllies and then the entire barbox package

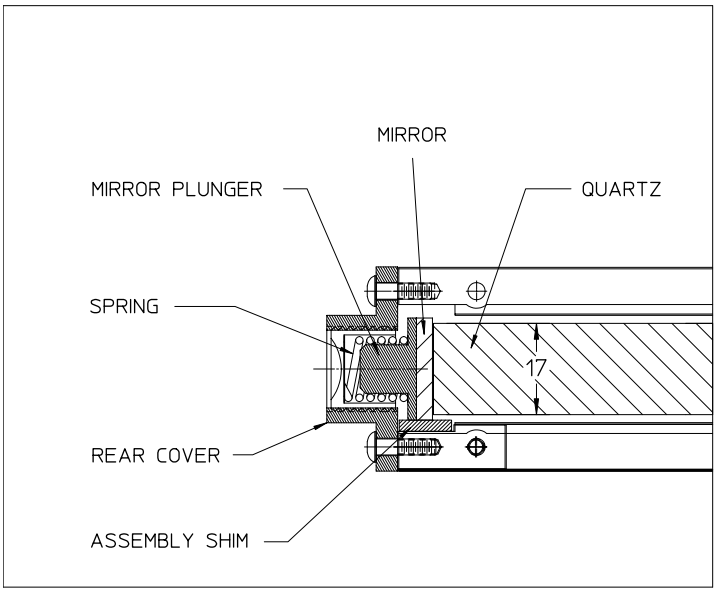

Figure 12: Crossection through the mirror end of a barbox, showing the end of the radiator bar, front surface, aluminum on quartz mirror, and spring plunger

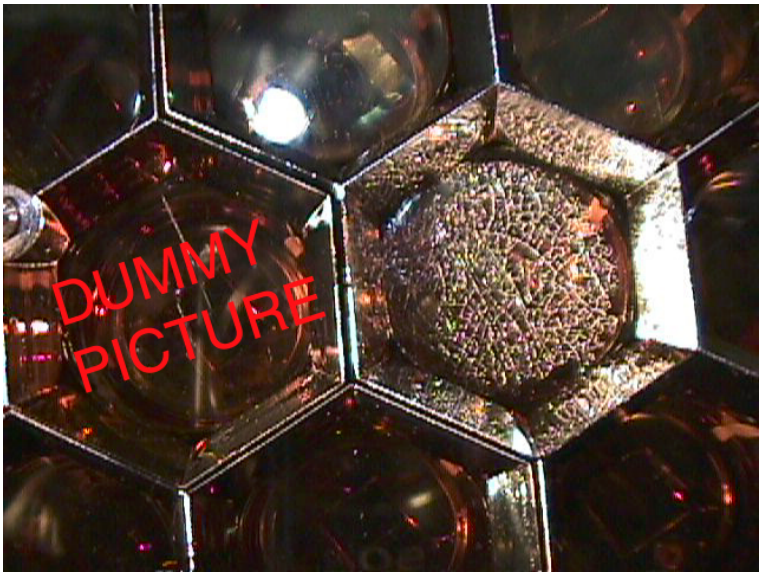

Figure 13: Detailed end view of the window of a barbox showing the window-frame, fuzed silica window and three wedges and its proximity to the nearest neighbor.

was shipped from the construction area at LBNL to the clean room at SLAC in one of two special containers, each capable of holding four barboxes.

5 Quartz Gluing and BarBox Assembly

The mechanial design of the barboxes has been previously described. In this section the gluing of the individual quartz components into final assemblies is discussed, as well as their installation into the barboxes, with short descriptions of the special fixtures necessary to complete the assembly process.

5.0.5 Gluing Alignment Fixtures

The five components of a long-bar, a wedge and four short bars, must be precisely aligned during gluing so the long-bar assemblies can be laid next to each other inside the barbox with only $\sim 150\mu$m separting the long bars over their 4.9 meter length. The angular infromation of the reflected Cherenkov light is preserved by minimizing angular mis-alignments of the bars, and the bars are parallel in z to typically less than 20 μrad.

The gluing process is complicated by the fact that the epoxy glue [6] chosen used takes 48 hours to cure, so the bars must be securely held at nearly constant temperature and orientation for two days for each gluing cycle (three gluing cycles are required per long bar, see below). The glue joint between two short-bars or short-bar to wedges is set to be 25 μm thick. Tension tests of sample glue joints indicated that at this thickness the glue joint was stronger than the quartz ($\geq$ 6.8 MPascal or 1000 psi). In all glue joints between bars (or bar to wedge joints) the glue is introduced into the joint by applying a few drops on top of the joint and allowing capilliary action to draw the glue into the void between parts. Typically it takes of order one hour for the glue to flow completely into the joint. After 8-10 hours, the excess glue is removed. The joints are cleaned after 24 hours of curing, and the glue is completely cured after 48 hours. During this 48 hour process, it is imperitive that the space between the bars be held at 25 μm. Although the clean room temperature is typically held to $\pm 2^{\circ}$C, even this temperature variation could open the joints by 50 μm due to the differential expansion of the quratz bars and the gluing table. Hence, in any set (or sub-set) of bars being assembled there is only one "active" glue joint at a time, and the bars are only clamped longitidionally directly next to the "active" joint.

It is critical that the bar surfaces not be damaged by contact with metal parts, consequently the fixtures used to align the bars were manufactured so that only plastic bumpers (typically nylon or teflon) came into contact with the bar surfaces.

The first glue step involves gluing the wedge to the end of a short bars. This is done in a set of six specialized glue fixtures, so two glue cycles are necessary to to produce 12 wedge-short bar assemblies. The next two glue cycles involved gluing the short-bars together to form long-bars. During these two glue cycles the short-bars are clamped in two duplicate sets of gluing fixtures, each set capable of simultaneoously holding seven long-bars. Within each set of glue fixtures, there is an array of 2×7 clamps at each three joints necessary to glue 28 short bars into seven long bars.

All gluing fixtures are mounted on a six meter long optical table and all 12 long-bars per boxbox can be glued during the same gluing period, with room for two spares.

Fig. 14 shows an example of several bars clamped into a gluing station. The vertical height of the fused silica bars at the glue joint were defined by plastic bumpers that were glued into the fixture, then ground to a common height $\pm 3\mu$m. The bars are clamped vertically at the joint during gluing. Small ($\sim 25\mu m$) mis-allignments can be tolerated if they are common to all bars, as long as the bars "nest" together inside the barbox. Hence the following two step strategy was developed

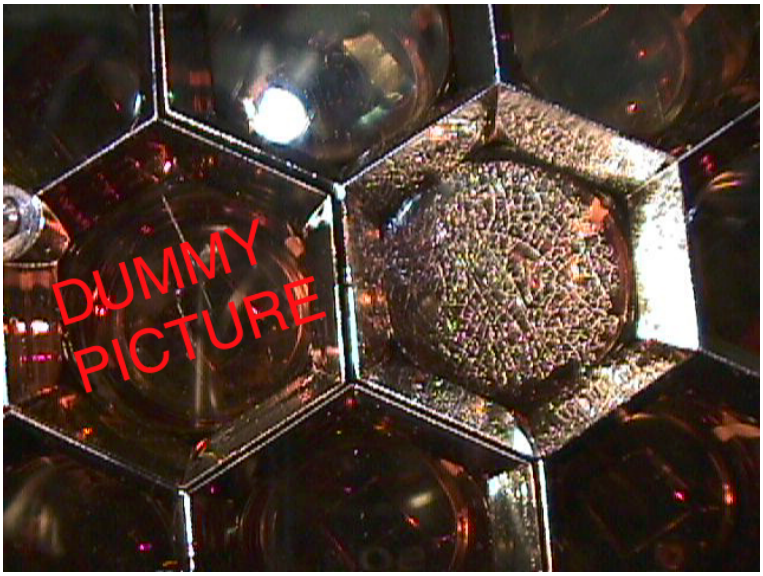

Figure 14: A picture of several bars clamped into the glue station.

to fabricate the glue fixtures: 1) the plastic bumpers that locate the bars tranverse to their length were glued into the fixtures by pressing them against a template manufactured to $\pm 2.5 \mu m$. All glue stations were manufactured using the same template, so any small, residual errors in the template are common to all joints. A solid joint between the nylon bumpers and the aluminum substate of the fixtures was guaranteed by using threaded nylon rod for the bumpers, the latter rounded at the end in contact with the fused silica.

Once these bumpers were glued into the individual clamping fixtures, the second step is to align the clamping fixtures on the gluing table. These fixures were aligned over the 4.9 meter length of the long bar assemblies by positioning them under a microscope with a tensioned 100μm diameter tungsten wire stretched the length of the table acting as a straight edge. A subsequent suvey of the fixtures using traditional optical survey equipment could not find any deviation from straightness to the level of presision of the survey of $\sim 25 \mu m$.

5.0.6 Installation of Long Bars into the Barbox

Once 12 long-bars were glued together, the next step was to insert them into the barbox. The construction of the barboxes, and the pricipals of the support of the fused silica bars within the barbox has already been discussed. A written procedure

was followed for the bar installation, and critical as-built dimenensions were recorded for later input into the detector geometry and comparison with results obtained from colliding beam data.

The barbox was prepared by adjusting the barbox on a transport frame resting on a granite table. The barbox was leveled to $\sim 25\mu m$ at a matrix of eight locations along its length and two locations accross its width (16 total points) with respect to the surface of the granite assembly table. Next the eight side load buttons were adjusted to the appropriate depth, based on the measured total width of the fused silica bars intended for that box. These buttons were brought into alignment with each other by adjusting them with respect to a tungsten wire stretched the full length of the barbox. At the wedge end of the barbox a set of 12 dial indicators were positioned that were used to measure the longitudional position of the bars. The barbox was then ready to accept bars.

The first operation was to transfer the individual long-bars about three meters from the gluing table to the assembly table. This was accomplished by a custom, light weight crane that ran on two trollies suspended from the ceiling. The crane attached to the long bar via the 4×2 plastic holders that had been applied to each individual short-bar as part of their initial quality control. Once the bar was transferred to the assembly table, these plastic holders were removed. The bars were lifted by hand (4 persons working together) cradling the bar with eight mylar strips as it was lifted from the table and into the barbox. This bar was then pushed $\sim$ 40mm latterally against the eight fixed side load buttons, where it is trapped above and below by the side extrusion of the barbox. Finally, the long bar was adjusted by hand in longitudional position so the $32 \times 91\ mm^2$ face of the wedge was in the correct location to $\pm 12\mu m$.

The second bar was inserted into the barbox in a similar fashion to the first bar, except that prior to pushing it against the first bar, it was equiped with the eight custom shims to establish the gaps between itself and its two nearest neighbors. These shims were located a the same point along the bar length as the fixed side supports, so that there were no bending moments due to offset supports. The nominal shim thickness was $150\mu m$, made from a piece of 50μm thick aluminum foil cut in the shape of an "H", where the cross bar of the "H" is slightly larger than the 35mm width of the bar. The two legs on each side of the "H" are each folded over to form a $150\mu m$ shim, while the cross bar of the "H" supports the shim accross the top of the bar, similar to "ear muffs". Thicker shims could be made by using thicker aluminum foil, or by inserting descrete shims into the folded aluminum shim package.

Ideally, all four bars used to construct a single long-bar were to have the same

35mm transverse dimentions to $\pm 25\mu m$. Operationally, however these tolerances were not held by the manufacturer, and the width of each bar had to be measured and a custom shim fabricated to fit. The widest bars were used in the fiducial volume of the detector, and the narrower bars were used close to the readout end. This approch kept the full fiducial coverage of the detector, at the cost of slightly reduced ($\sim$ 3%) light yield. To allow for variable width short-bars in the same long-bar assembly, the width of each short bar was measured and stacks of spacers, up to 1 mm thick, were added to nominal $150\mu m$ aluminium shims between bars to account for the missing material.

The rest of the bars were inserted in a similar fashion in the following order from the reference edge: 1, 2, 3, 4, 5, 6, 7, 8, 9, 12, 11, 10. The order of the last three bars is inverted, because the 12th is trapped by side extrusions and cannot be installed from above. There was adequate space in the Barbox to insert the last bar (10, from the reference edge), and still remove the mylar strips used to support it as it is moved from the table top into the Barbox without disturbing the shims already installed on bar 11.

After all twelve bars were inserted into the Barbox, the side load buttons opposite the reference edge were slightly tightened. At this stage, a $75\mu m$ shim was passed in the gaps between all the bars to insure they were not touching.

Next, the front surface mirrors were applied to the ends of the bar opposite the wedges. Each mirror was temporally held with two drops of UV curing glue [7] at the top edge.

After all twelve mirrors had been "tacked" to the bars in this fashion, the end cover of the Barbox was installed, and the spring-loaded end plungers were lightly tightened against the mirrors to hold them in place.

The top cover was then applied. A final check of the longitudinal position of the wedge faces is made, and bars out of position by more than $\pm 12\mu m$ were adjusted. With the top cover installed, the side load are tightened to their final load (a total of 1.5 times weight of the bars in each direction). If any bar moved more than $\pm 12\mu m$ during this process, the side load buttons were loosened, and the bar repositioned. This procedure never had to be repeated more than three times, and was successful on the first try about half the time. After tightening the side load buttons, the top load buttons were tightened equalising the vertical load on the bars according to an algorithm that included the bending of the cover. Typically tightening these top-load buttons did not cause the bars to shift longitudinally.

Twelve bars could be inserted into the Barbox in about seven hours, including one hour to install the mirrors and two hours to install the top of the Barbox and adjust the top load buttons.

5.0.7 Window Gluing

At this point the 12 long-bars have been installed in the Barbox, the mirror opposite the wedges installed and the bars are adjusted to $\pm 12\mu m$ in longitudinal position. The most difficult task in assembling the Barbox was gluing the fused silica window simultaneously to the twelve wedges at the readout end of the bars. The procedure was developed over three months of testing with glass and natural quartz substitutes, and depended critically on the cleanliness of the window, as described in the fused silica quality control section of this paper. Dust or residue on the window or wedge surfaces would prevent the glue from flowing properly and lead to bubbles in the glue joint.

Using a custom fixture, the wedges are pushed up or down so that their front surface was perpendicular to the surface of the granite table, as measured by pair of dial indicators that had been previously adjusted using a precision square. Again the tolerance on the perpendicularity of the wedge faces to the table was $\pm 12\mu m$. After the wedges had be adjusted for perpendicularity, the indicator fixture was removed, and the window frame components installed. The window frame components were leveled with respect to the Barbox, and became part of the fixture for gluing the window to the wedges.

The specially cleaned window was positioned next to the faces of the wedges using extension rods that supported the window from the frame. The window was spring loaded against the twelve wedges with a set of six $75\mu m$ shims separating them (two shims on each end, and a pair at the edge near the center of the window). The window was placed at a known height with respect exterior of the window frame, and centered horizontally on the frame with shims whose thickness was calculated from the "as-built" dimensions of the window.

Using the same epoxy glue [6] and similar technique as for the bar-to-bar joints, drops of glue were applied to the top of the twelve wedges, and the glue allowed to flow down between the wedge faces and the common window via capillary action. During this process it was imperative that the glue not form a joint between neighbouring wedges, so that light would not leak from one wedge via misplaced glue into a neighbouring wedge. For this reason, the wedges were typically 2 mm narrower than the bars, and capillary action between wedges was defeated.

After the glue had flowed from the top to the bottom of the wedges (about 1.5 hours), the $75\mu m$ shims between the window and wedges were removed, and the window sucked by the surface tension of the glue to within $25\mu m$ of the wedges. Tests of the strength of this glue joint using this procedure indicated it was as strong as the bar-to-bar joints, where the $25\mu m$ glue thickness was enforced by clamps: *i.e.*

the joint was not starved for glue. After the shims were removed, the excess glue was removed about 8 hours later, and the glue was allowed to cure for a total of 48 hrs. Typically, each wedge glue joint would have zero to three small bubbles over the $32 \times 91\ mm^2$ surface, each bubble about $10 - 15\mu m$ in diameter.

There after the window frame was applied to the window, and covers were glued between the window frame and the rest of the Barbox.

5.1 Bar Loading and Gas Sealing

After the epoxy holding the window frame elements had cured, the spring plungers on the the mirror end of the bars were tightened to a load of 150 kgf. The gas connections to the Barbox were installed, in particular, a 3 mm diameter supply line that ran from the wedge end to the mirror end was glued into pre-machined holes in the forward and rear assemblies.

All screw adjustments penetrating the Barbox were covered with aluminium strips and sealed with epoxy glue [8] to prevent gas leaks. The gaps between the cover and the body of the Barbox were sealed from the outside with epoxy. The integrity of the Barbox was tested by filling it was gas, and requiring it hold a pressure of 12 mm water column equivalent.

Opening a fully sealed Barbox is considered a destructive operation, and it is unlikely the mechanical parts from an opened Barbox could be salvaged. Parts for two spare Barboxes were constructed.

The assembly process from gluing the bars together to final gas sealing of a Barbox could be completed in about 13 working days, including eight days to make up the wedge-to-bar and bar-to-bar joints. Gluing of the wedges for and bar-to-bar joints one Barbox could proceed partially in parallel with the assembly of a previous Barbox, so that at full tilt, about one Barbox per week could be assembled. In fact, the construction of the Barboxes was always limited by the supply of the short-bars from the vendor.

5.2 Barbox Installation into BaBar

Once the Barboxes had been assembled with the fused silica bars at SLAC, they were stored on special racks in a temperature controlled environment until they were needed for installation. Transfer of the Barboxes from the clean room to the storage facility was accomplished with a specially constructed A-frame crane, using a custom lifting fixture that encircled the Barboxes at an array of 2×5 points along its length.

Barboxes in lowest section of the detector (4-7) had to be installed before the detector was moved onto the beam line, because their installation conflicts with the fixed concrete supports of the accelerator components. The other Barboxes can be installed on beam line, and this was actually done for the upper six Barboxes.

Once a specified Barbox was identified for installation, it was removed from the storage facility using a fixture that would eventually double as the installation fixture for the Barboxes into the BaBar detector. This fixture would allow the Barbox to be rotated to the same plane as the slot in the support structure, incorporated a rail system to support the Barbox as it was slid into the slot, and a laser alignment system (see below).

The Barboxes were transported from the storage facility to the BaBar detector, about 1/2 kilometer away, using a standard, motor driven crane.

Installation of the upper eight Barboxes was complicated by the presence of the accelerator components, which for some Barboxes came within 1cm of the path of the Barbox. The installation fixture was held above the accelerator components using a cantilevered support arm, as shown in Fig. 15. The installation arm could move transversely to the beam, raise or lower the Barbox, and provided a point of support about which the Barbox could be rotated to match the azimuthal angle of the Barbox slot.

Prior to installation, the beam from a He-Ne laser mounted at the back of the installation fixture (*i.e.* the end furtherest from the IP) was aligned with the rails on the installation fixture using a target that moved along these same rails. Thereafter, a mirror was mounted on the face of the Assembly Flange (see Fig. 1) that was used to align the tracks of the installation fixture perpendicular to the face of the Assembly Flange as follows: a) the Barbox was rotated in ϕ, and adjusted in $x - y$ until its forward end was centered with and parallel to the Barbox slot into which it was to be inserted and b) the height and transverse location of the rear Barbox was adjusted until the beam from the laser mounted at the rear of the installation fixture reflected from the mirror mounted on the assembly flange came straight back to the laser. At this point the Barbox could be slid from the rails of the installation fixture into the Barbox slot, were the load was taken up by the Barbox wheels that ride on tracks of the support structure.

During Installation, the z location of the barbox inside the support structure was determined by a temporary, special stop that fastened to the barbox via the gas inlet. As described above the pressure of the SOB water on the window corresponds to a force of 150 kgf for the lower barboxes, and this force must be resisted via a connection between the back of the wedge cover and the assembly flange of the support structure. Due to fabrication tolerances the gap between the wedge cover

Figure 15: Installation of a barbox into the BaBar detector. Not seen in the figure is the cantilevered support arm which supports the installation fixture above the accelerator components.

and the assembly flange can vary by several mm, and the two surfaces are not perfectly parallel. To create a solid joint between the assembly flange and the wedge cover a 6mm high (Δr) by 400 mm wide ($r\Delta\phi$) "putty-like" epoxy [9] was applied to the back of the wedge cover, and then this material was compressed as the barbox was pushed into its slot against the stop just described.

Once the Barbox was installed into its slot and the epoxy support allowed to cure (approximately 1 hr), the water seal was made up and the gas system connected. About two Barboxes per day were inserted into the detector.

5.3 DIRC Gas System

Dry nitrogen gas from liquid nitrogen boil-off flows through each box at the rate of 150 cc/min , and is monitored for humidity to ensure that all boxes remain tightly sealed. The gas is filtered through a molecular sieve and three mechanical filters to remove particulates (7μm, 0.5μm and 0.01μm). Typical dew points on the gas exhausted from the Barboxes are on the order of -40°C, although one Barbox has a consistently higher dew-point of -26°C with an enhanced N_2 flow rate. About one third of the input N_2 gas leaks from the Barboxes and keeps the Barbox slots in the mechanical support structure free of condensation.

Potential leaks from the water seals between the Barboxes and the stand off box are detected by a water leak detection system of 20 custom water sensors in and about the Barbox slots, two commercial ultrasonic flow sensors to monitor water flow in two (normally dry) drain lines in addition to the twelve humidity sensors on each of the twelve N2 gas output lines. The custom water sensors consist of a pattern of interdigitated copper lines printed on kapton foil, shorted by a 3 MΩ resistor at the end of 15m of cable. The nominal loop current of 1 micro amp is monitored, with higher currents indicating the presence of water and lower currents indicative of a fault condition.

Logically, each Barbox is monitored by 4 different water sensors (some water sensors are shared between Barboxes for mechanical reasons). A majority logic system based on the input from the 34 water and humidity sensors determines if the water in the Standoff Box should be released. A water dump is initiated if 2 out of 4 sensors (selectable from 1/4 to 4/4) corresponding to the the *same Barbox* indicate the presence of water. The system is connected to the BaBar UPS system, and in the event of this power fails, no action is taken. Should water be detected a valve in a 10 cm diameter drain line is opened, and the water can be drained in about 12 minutes.

References

[1] "FEA Analysis of the DIRC Structure", MCR Associates, Inc., 111 W. Evelyn Ave, Sunnyvale, CA 94086, 10/15/96.

[2] Araldite 2011, Ciba-Geigy, 4917 Dawn Ave., East Lansing, MI 48823.

[3] Hysol EA 9360, Hysol Aerospace Products, 2850 Willow Pass Road, Pittsburg, CA 94565.

[4] Hysol EA 9359.3, Hysol Aerospace Products, 2850 Willow Pass Road, Pittsburg, CA 94565.

[5] Scotch Weld DP-190, 3M Industial Specialties Division, St. Paul, MN 55144.

[6] Epotek 301-2, Epoxy Technology, 14 Fortune Drive, Billerica, MA 01821.

[7] UV curing adhesive, type 63, Norland Products, 695 Joyce Kilmer Ave, New Brunswick, NJ 08901.

[8] Hysol 1C-LV, Hysol Aerospace Products, 2850 Willow Pass Road, Pittsburg, CA 9455.

[9] Araldite AV 1580 GB and hardner HV 1580 GB, Ciba-Geigy, 4917 Dawn Ave., East Lansing, MI 48823.